Biogeosciences Discuss., https://doi.org/10.5194/bg-2019-49
Manuscript under review for journal Biogeosciences
Discussion started: 12 February 2019

El Niño–Southern Oscillation (*ENSO*) event reduces CO_2 uptake of an Indonesian oil palm plantation

Christian Stiegler[1], Ana Meijide[2], Yuanchao Fan[3], Ashehad Ashween Ali[1], Tania June[4], Alexander Knohl[1]

[1]Bioclimatology, University of Goettingen, Goettingen, Germany
[2]Department of Crop Sciences, Division Agronomy, University of Goettingen, Germany
[3]NORCE Norwegian Research Centre, Bjerknes Centre for Climate Research, Bergen, Norway
[4]Department of Geophysics and Meteorology, Bogor Agricultural University, Bogor, Indonesia

Correspondence to: Christian Stiegler (christian.stiegler@biologie.uni-goettingen.de)

Abstract. The El Niño–Southern Oscillation (*ENSO*) in 2015 was one of the strongest observed in almost 20 years and set the stage for a severe drought and the emergence of widespread fires and related smoke emission over large parts of Southeast Asia. In the tropical lowlands of Sumatra, which were heavily affected by the drought and haze, large areas of tropical rainforest have been converted into oil palm (*Elaeis guineensis* Jacq.) plantations during the past decades. In this study, we investigate the impact of drought and smoke haze on the CO_2 exchange, evapotranspiration and surface energy budget in a commercial oil palm plantation in Jambi province (Sumatra, Indonesia) by using micrometeorological measurements, the eddy covariance method and a multi linear regression model (*MLRM*). With the *MLRM* we identify the contribution of meteorological and environmental parameters to net ecosystem CO_2 exchange. During the initial part of the drought, when incoming shortwave radiation was elevated, CO_2 uptake increased by 50% despite a decrease in upper-layer soil moisture by 35%, an increase in air temperature by 10% and a tripling of atmospheric vapour pressure deficit. Emerging smoke haze decreased incoming solar radiation by 35% compared to non-drought conditions and diffuse radiation became almost the sole shortwave radiation flux for two months resulting in a strong decrease in CO_2 uptake by 86%. Haze conditions resulted in a complete pause of oil palm carbon uptake for about 1.5 months and contributed to a decline in oil palm yield by 35%. With respect to climate change and a pronounced drying trend over the western Pacific during El Niño, our model showed that an increase in drought may stimulate CO_2 uptake while more severe smoke haze, in combination with drought, can lead to pronounced losses in productivity and CO_2 uptake highlighting the importance of fire prevention.

1 Introduction

El Niño – Southern Oscillation (*ENSO*) is a coupled ocean-atmosphere interaction phenomenon in the equatorial Pacific Ocean and one of the most distinct drivers of seasonal to interannual regional and global climate variability (Wolter & Timlin, 2011). Increasing sea surface temperatures in the eastern and central tropical Pacific Ocean are linked to increases in sea-level air pressure in the western Pacific Ocean resulting in reduced cloudiness and low precipitation over Southeast Asia (Rasmusson

& Carpenter, 1981; Wolter, 1986). Generally, *ENSO* shows episodic and varying timing, frequencies and amplitudes but *ENSO* during 2015 was the strongest observed in almost 20 years (Santoso et al., 2017; Lim et al., 2017). It set the stage for a severe drought over large parts of Southeast Asia, particularly in Indonesia, which favored the emergence of widespread and mostly human-induced forest, grassland and peat fires (Betts et al., 2016).

The fires released record-breaking amounts of terrestrial-stored carbon as CO_2 into the atmosphere, with mean daily emission rate of 11.3 Tg CO_2 during September to October 2015 (Huijnen et al., 2016). The recent *ENSO* elevated Mauna Loa mean monthly CO_2 concentration for 2015 above 400 ppm for the first time in its measurement history and contributed to the highest annual CO_2 growth rate on record (Betts et al., 2016). The emitted aerosol particles from biomass burning covered large parts of Sumatra, Borneo, Malay Peninsula and Singapore for several months under a persistent pall of smoke haze.

The regions affected by the smoke haze, especially Indonesia and Malaysia, have undergone substantial land-use changes within the past two decades due to the world's hunger for cheap vegetable oil, such as palm oil (Koh et al., 2011). Oil palm (*Elaeis guineensis* Jacq.) emerged to an important cash crop due to the extensive application of palm oil in pharmaceutical, cosmetics and food industries as well as for biofuel (Koh & Ghazoul, 2008; Turner et al., 2018). Indonesia and Malaysia are the world's biggest producers of palm oil. For example, in 2016/17, the two countries contributed 56% (Indonesia) and 30% (Malaysia) to the global supply of palm oil (USDA, 2018). In 2015, oil palm plantations in the two countries combined covered 17 Million hectares (Chong et al., 2017).

Oil palm has high average life span of >25 years (Woittiez et al., 2017) and is adapted to tropical climate with optimal mean temperature of 24-28°C, it requires frequent and sufficient precipitation of ~2000 m yr^{-1} and high level of solar radiation (Bakoumé et al., 2013; Corley & Tinker, 2016). Oil palm shows distinct reaction to changes in atmospheric and soil parameters, with gradual symptoms of water and heat stress such as inhibited growth (Legros et al., 2009; Cao et al., 2011), snapping off leaves and drying out of fruit bunches (Bakoumé et al., 2013), reduction in yield (Caliman & Southworth, 1998; Noor et al., 2011), reduction or even pause in carbon dioxide assimilation (Rivera Méndez et al., 2012; Jazayeri et al., 2015) and ultimately, plant death (Maillard et al., 1974).

Aerosol particles from biomass burning generally reduce the amount of sunlight reaching the surface and increase the fraction of diffuse radiation through scattering (Kozlov et al., 2014). Diffuse light conditions enhance plant photosynthesis and evapotranspiration through more uniform through-canopy distribution of photosynthetically active radiation (*PAR*) (Knohl & Baldocchi, 2008; Kanniah et al., 2012; Heuvelink et al., 2014). Light haze smoke intensities may therefore increase CO_2 uptake, maximum rate of photosynthesis (A_{max}) and evapotranspiration but during dense haze smoke, the effect is reversed and high share of diffuse light may strongly reduce both CO_2 uptake and evapotranspiration (Yamasoe et al., 2006; Moreira et al., 2017). In addition, ambient atmospheric CO_2 increase due to local fires and burning may act as a temporary plant CO_2 fertilization which, to some extent, may offset reduced plant CO_2 uptake during dense smoke haze (Mathews & Ardiyanto, 2016).

Global warming and consequent regional climate changes, including changes in precipitation pattern and increase in the magnitude and frequency of extreme events such as drought, *ENSO* and fires (Neelin et al., 2006; IPCC, 2013; Jiménez-Muñoz

et al., 2016), may severely stress oil palm plantations (Tangang, 2010; Rowland et al., 2015). It is therefore important to assess how much *NEE* would change under such conditions. Model predictions suggest more intense *ENSO* over the course of the 21st century, which may result in a general drying in the western regions of the Pacific Ocean during El Niño (Power et al., 2013; Cai et al., 2014; Kim et al., 2014; Keupp et al., 2017; Cai et al., 2018). Increasing frequency of *ENSO*-related drought in Southeast Asia has already caused a decline of 10-30% in palm oil production (Paterson et al., 2017). Projected temperature increase and water stress through enhanced *ENSO* might further decrease oil palm yield (Oettli et al., 2018) or even lead to detrimental conditions for oil palm growth in some areas in Southeast Asia (Paterson et al., 2017). On the other hand, *ENSO* is associated in Indonesia with an increase in incoming solar radiation which can increase CO_2 uptake in a tropical environment (Olchev et al., 2015). However, current studies and modelling approaches lack a holistic understanding of ecosystem response, resilience and the underlying meteorological, ecological and biological processes during extreme events, such as drought and smoke haze conditions. The *ENSO* in 2015 was the first strong climate extreme event after the major land-use conversions on Sumatra from forest into oil palm plantations but only little is known about how the *ENSO*-related severe drought and persistent smoke haze influenced oil palm monoculture.

In this study, we therefore aim to (a) quantify land-atmosphere CO_2, water vapour and turbulent heat exchange over oil palm plantation using the eddy covariance technique during the 2015-*ENSO*, (b) analyse the contribution to net ecosystem CO_2 exchange (*NEE*) of meteorological and environmental parameters using a multiple linear regression model (*MLRM*), (c) investigate the impact of a possible future more severe drought and smoke haze scenario on *NEE* and (d) evaluate potential changes in evapotranspiration and energy fluxes to the atmosphere. We hypothesize that (a) oil palm monoculture would reduce net ecosystem CO_2 uptake and maximum photosynthetic rate (A_{max}) during drought and haze, and (b) sensible heat fluxes would increase at the cost of evaporative cooling.

2 Materials and methods

2.1 Study site

The study site is located in a commercial oil palm plantation (1°41'35.0"S, 103°23'29.0"E, 76 m a.s.l.) in tropical lowlands of Jambi province on Sumatra island (Indonesia), approx. 25 km west-southwest of Jambi City (Figure 1). The landscape is flat with small elevation variations of approx. ± 15 m. Average mean annual air temperature during the period 1991-2011 is 26.7°C (± 0.2°C standard deviation) and mean precipitation for the same period is 2235 mm yr-1 (± 381 mm SD), with a dry season from June to September and two peak rainy seasons around March and December (Drescher et al., 2016). Long-term climate records are collected at Sultan Thaha Airport Jambi, approx. 29 km east-northeast of the study site. The oil palm plantation covers 2186 ha and the palm seedlings were planted in the years 1999, 2002 and 2004. Our measurements are located in the section where the palms have been planted in 2002. Average palm height in 2014 was 12 m and leaf area index (*LAI*) was 3.64 m2 m-2 (Fan et al., 2015). Palms are planted in a triangular array, with 8×8 m horizontal density. In 2015, 144 kg ha^{-1} of Magnesium Nitrate, 575 kg ha^{-1} of NPK Granular, and 251 kg ha^{-1} of Dolomite fertilizers were applied in topdress application.

The plantation is owned by Perseroan Terbatas Perkebunan Nusantara VI, Batang Hari Unit (PTPN6). Stumps of pruned oil palm leaves are densely covered with epiphytes, e.g. ferns (*Polypodiophyta*) or flowering plants (*Melastomataceae*, *Orchidaceae*), while understory vegetation is scarce due to regular application of herbicides and occasional mowing. Highly weathered Loam Acrisols soils dominate in the area (Allen et al., 2015) and mean soil carbon and nitrogen content in the plantation reach 1.12% (± 0.34% SD) and 0.08% (± 0.02% SD) (Meijide et al., 2017).

2.2 Eddy covariance measurements

Eddy covariance (*EC*) measurements to derive fluxes of sensible (*H*) and latent (*LE*) heat, CO_2 net ecosystem exchange (*NEE*) and water vapour (*ET*) for this study were carried out from June 2014 to July 2016. We use a LI7500A fast response open-path CO_2/H_2O infrared gas analyser (LI-COR Inc. Lincoln, USA) and a Metek uSonic-3 Scientific sonic anemometer (Metek, Elmshorn, Germany). The *EC* system measures at 10 Hz and is placed at the top of a 22 m high steel framework tower. Digital signal recording, statistical tests for raw data screening and raw data correction, spectral analysis, eddy flux calculation using EddyPro (LI-COR Inc, Lincoln, USA), post-processing such as quality flagging, removal of fluxes during stable atmospheric conditions, i.e. friction velocity (u*) <0.1 m s-1, flux footprint analysis and gap filling of missing flux data follow standard procedures (Meijide et al., 2017). The energy balance closure for the entire study period was 0.75 (R^2 = 0.85).

2.3 Meteorological ad environmental parameters, oil palm yield

Above-ground measurements include air pressure (22 m above the surface), precipitation (11.5 m), wind direction (15.4 m) and wind speed (18.5, 15.4, 13 and 2.3 m), air temperature and air humidity (22, 16.3, 12.3, 8.1, 2.3 and 0.9 m), incoming and reflected photosynthetically active radiation (*PAR*) (22 m), incoming and outgoing shortwave and longwave radiation (22 m), global and diffuse radiation (22 m), and sunshine duration (22 m). Detailed information on instrument type and manufacturer for all measured parameters can be found in Meijide et al., (2017). Below-ground measurements consist of three profiles where ground heat flux (*G*) is measured with heat flux plates at 5 cm depth and soil moisture and soil temperature is measured at 0.3, 0.6 and 1 m depth, respectively. All meteorological and environmental parameters were measured every 15 s and stored as 10-minute mean, minimum and maximum values in a DL16 Pro data logger (Thies Clima, Göttingen, Germany). Monthly oil palm yield data was provided by PTPN6 and covers the period January 2013 to April 2017.

2.4 Data analysis and statistics

The meteorological data used in this study covers the period from May 2014 to July 2016. Based on precipitation and the ratio between diffuse and global radiation (R_G), i.e. fraction of diffuse radiation (*fdifRad*), we defined four distinct meteorological periods during 2015, i.e. pre-drought, non-haze drought, haze drought, and post-haze and compared the four periods with meteorological conditions in 2014 and 2016. We consider pre-drought as the period with frequent precipitation on an almost daily basis and non-haze drought as the period when precipitation occurred only sporadically and heavy precipitation events >50 mm d^{-1} were completely absent. Haze drought period follows the non-haze drought. We defined the start of the haze

drought period at the day when daily average fraction of diffuse radiation was >0.8 for more than three consecutive days. We consider the end of the haze drought period as the day when daily average fraction of diffuse radiation dropped below 0.8 for five consecutive days and when clear day-to-day variations in fraction of diffuse radiation, with day-to-day variation of >0.2 became apparent. Reference meteorological conditions cover the period May-December 2014 and January-July 2016.

Maximum rate of photosynthesis (A_{max}) at ecosystem scale was calculated from daily light response curve (Falge et al., 2001). In this study, we assign *H*, *LE* and *NEE* as positive when they are directed away from the surface. To avoid negative values of A_{max} and for better readability, we perform sign conversion of A_{max}. All statistical analyses and graphing were performed with R version 3.1.1 (R Core Development team, 2014).

2.3 Multiple Linear Regression Model

We used a multiple linear regression model (*MLRM*) (Ray-Mukherjee et al., 2014; Whittingham et al., 2006) to investigate the temporal contribution of climatic variables to observed trends in *NEE*. The first *MLRM* used in this study considered the diel averaged *NEE*, which includes both the photosynthetic and respiratory processes. We built the model including vapour pressure deficit (*VPD*), atmospheric CO_2 concentration (CO_2), fraction of diffuse radiation (*fdifRad*), wind speed (*wind*), air temperature (*tair*) and actual evapotranspiration divided by potential evapotranspiration (*ET_ET_pot*). Unless otherwise stated, the environmental variables used in this study are measured above the canopy in 22 m height. The form of the model for the 24-hour averaged *NEE* is as follows:

$$NEE = \beta_1 VPD + \beta_2 CO_2 + \beta_3 fdifRad + \beta_4 wind + \beta_5 tair + \beta_6 ET\_ET\_pot \quad (1)$$

where β is the slope. We did not include the intercept term in equation (1) because without the intercept the model gave a relatively high goodness of fit (see Supplement, Table S1). Our first criteria of the model design (equation 1) was to ensure that the β's are highly statistically significant (Chatfield, 1995). Our second criteria of the model design (equation 1) was to choose the predictors in such a way so that they are least correlated (Zuur et al., 2010). We also standardized the data to consider normality and non-linearity (Chen et al., 2018), but these changes reduced the goodness of fit by a large amount. Therefore, throughout this study we use the data in the original form. In the initial model setup (equation 1), we included predictors that are more closely related to drought such as precipitation and soil moisture at different depths, but these predictors were not significant (p-value >0.1). Thus, we excluded them from the model and used only predictors which were highly significant.

For the second *MLRM*, we focused on the midday *NEE* (10-14 h local time), which is dominated by photosynthesis and thus avoids any issues of nighttime flux uncertainties. In this case, we used predictors for our model which were significant, i.e. incoming photosynthetically active radiation (*PARin*), *tair*, *VPD*, CO_2 and *fdifRad*. The form of the model for the day-time *NEE* is as follows:

$$NEE = \beta_1 PARin + \beta_2 tair + \beta_3 VPD + \beta_4 CO_2 + \beta_5 fdifRad + \beta_6 ET\_ET\_pot \quad (2)$$

To complement day-time *NEE*, we looked as well at night-time *NEE* (19-5:30 h local time). The modeled *NEE* for the night-time takes the following form:

$$NEE = \beta_1 tair + \beta_2 VPD + \beta_3 ET\_ET\_pot + \beta_4 tair_{12} + \beta_5 wind \quad (3)$$

For the nighttime *NEE*, we also considered environmental variables within the canopy profile, i.e. air temperature measured at 12 m above the soil (*tair12*). In the night, soil respiration could be influenced by this environmental factor (Zhou et al., 2013). Initially, we also tested the model using soil temperature and soil moisture but these parameters were not significant.

2.3.1 *NEE* under intensified drought and haze conditions

We used the above three *NEE* models (equations 1 to 3) based on the 2015-drought and haze conditions to investigate the impacts of intensified non-haze drought (*NHD+*) and haze drought (*HD+*) conditions on oil palm *NEE*. Under intensified non-haze drought (*NHD+*), we expect an increase in *VPD*, incoming *PAR* and air temperature and a decrease in diffuse radiation. Thus, we modified the variables as *VPD* +20%, *fdifRad* -20%, *tair* +20%, *PARin* +20%, ET_ET_pot -20% and *tair12* +20%. Under intensified haze drought (*HD+*) we modified the mean environmental variables (*VPD* by +20%, CO_2 by +20%, *fdifRad* by +20%, *tair* by +20%, *PARin* by -20%, ET_ET_pot -20% and *tair12* by +20%) in the model.

3 Results

3.1 Atmospheric and environmental conditions

Strong inter-seasonal differences in precipitation pattern, air temperature and atmospheric *VPD* characterize the study period, with the year 2015 being slightly drier and warmer as during the reference periods of 2014 and 2016 (Table 1). From March 2015, both the daily mean air temperature and daily mean *VPD* showed a steady increase and reached their maxima during the haze drought period in mid-October (Figure 2). The first four months in 2015 were cooler and wetter than during the reference period (Table 1). From May until mid-September, when the non-haze drought hit the area in 2015, air temperature and *VPD* were of similar magnitudes in 2015 and the reference period but accumulated precipitation was as little as 192 mm in 2015 compared to 594 mm during the reference period (Supplement, Figure S1). Inter-seasonal differences in air temperature and in *VPD* were most pronounced from mid-September until mid-November, when haze covered the area in 2015. During that time, mean air temperature was 28.3 ± 0.8°C and mean *VPD* was 8.71 ± 2.57 hPa, which is 2.3°C and 4.98 hPa higher than during the reference period. There were sharp contrasts in soil water content (*SWC*) in 2015 between the pre-drought and haze drought period due to the absence of precipitation in the latter period. *SWC* in the upper two soil layers (30 & 60 cm) declined by 35%, respectively, while in the bottom layer (100 cm) the decline was 10% (Table 1). During the reference period,

differences in *SWC* were less pronounced, with maximum decline of 26% in the upper two soil layers. Daily mean global radiation and daily mean incoming photosynthetically active radiation (*PAR*) showed strong periodical and day-to-day variations over the course of the study period. In 2015, irradiance reached its maximum during the non-haze drought period in late July and mid-August (Figure 2). After this peak, the continuous emergence of haze led to a substantial decrease in both R_G and *PAR* (Table 1). Simultaneously, fraction of diffuse radiation increased from 0.21 to 0.99 and diffuse radiation remained almost the sole shortwave radiation component for almost two months. Compared to the reference period, daily average incoming *PAR* during the haze drought in 2015 decreased by 107 µmol m^{-2} s^{-1} (-36%) while fraction of diffuse radiation increased by 0.12 (13%) (Table 1). The persistence and density of the haze in 2015 is reflected in daily average sunshine duration (Table 1). During the haze drought period, the sun was, on average, visible for 50 minutes per day, which equals to 7% within 12 hours of potential daylight (sun above the horizon). During the pre-drought, non-haze drought and post-haze period, the sun was visible for 6.7 (56%), 10 (83%) and 6 (50%) hours per day, respectively. Atmospheric CO_2 concentration during the haze drought and post-haze period in 2015 was 5% (20 ppm) and 6% (24 ppm) higher than during the reference period.

3.2 Net ecosystem CO_2-exchange, carbon accumulation, yield and evapotranspiration

The oil palm plantation was a net sink of CO_2 during the study period. Mainly due to the impact of the haze period, net ecosystem CO_2 exchange (*NEE*) in 2015 (-1.79 ± 13.53 µmol m^{-2} s^{-1}) was significantly weaker ($P < 0.01$) compared to the reference period (-2.20 ± 14.48 µmol m^{-2} s^{-1}) (Table 2). Only in the very beginning of 2015 and during the period June-September 2015, *NEE* was higher compared to the reference period (Figure 3) and CO_2 uptake showed a slight increase coinciding with the drought-related increase in incoming *PAR*. The beginning of the haze drought marks a strong transition where CO_2 uptake initially decreased with developing haze, followed by a two-month period where the oil palm plantation turned into a small source of CO_2 to the atmosphere.

Carbon accumulation by the oil palm plantation was relatively strong in the first months of 2015 and exceeded accumulation of the reference period by up to 80 g C m^{-2} (Figure 3b). During the following months until mid-June, carbon accumulation of the reference period surpassed 2015-carbon accumulation but by mid-August these differences were offset. Due to the haze from October to mid-November 2015, carbon accumulation initially paused, followed by small overall carbon loss of 10 g C m^{-2} within 40 days. After the haze, the oil palm plantation was not able to offset the pause in carbon accumulation and carbon losses during the haze and therefore, the total amount of accumulated carbon in 2015 was 152.7 g C m^{-2} (18%) lower compared to the reference period (Table 1).

Over the course of the non-haze drought, the oil palm plantation reduced its maximum rate of photosynthesis (A_{max}) (Figure 4). However, drought-related changes in meteorological and environmental conditions caused a not relevant (3%) decrease in A_{max} compared to pre-drought conditions. With the continuous development of haze in September 2015 and related absence of direct sunlight the oil palm plantation seemed to compensate for the dim light conditions with a jump of A_{max} by 13 µmol m^{-2}

s^{-1} (37%) within a couple of days (Figure 4). This compensation effect of relatively high A_{max} continued over the haze drought period, with A_{max} being 4.8 µmol m^{-2} s^{-1} (18%) higher than during the non-haze drought.

Using linear regression between monthly *NEE* and oil palm yield, we found that a 6-month delay in yield showed highest R^2 of 0.36 ($P<0.01$) with *NEE*. Therefore, we consider the period November 2015 to May 2016 as the time when *NEE* and carbon accumulation during the non-haze drought and haze drought in 2015 were reflected in monthly oil palm yield. From August 2015, monthly oil palm yield declined continuously from 7950 t ha^{-1} to its minimum of 2128 t ha^{-1} in May 2016. Compared to the same period (Nov.-May) in the two years before and the year after the *ENSO* event, average yield affected by 2015-drought and haze was 32% (1421 t ha^{-1}) lower. Considering the 2015-haze drought only, average oil palm yield 6-9 months after the beginning of the haze drought was even 50% (2231 t ha^{-1}) lower compared to the non-*ENSO* years.

Total evapotranspiration (*ET*) derived from eddy covariance (*EC*) measurements was 1245 ± 362 mm yr^{-1} in 2015 and 1580 ± 469 mm yr^{-1} during the reference period (Table 2), with a higher share of *ET* on precipitation during the reference period (77.9%) compared to 2015 (64.5%). This observed difference was driven by the absence of precipitation during the non-haze drought period, which increased the overall share of sensible heating at the cost of *ET* (Bowen ratio) (Figure 5). In addition, oil palm drought and heat stress may have triggered partial stomata closure, which further decreased *ET* towards the end of the non-haze drought. The reduction in incoming solar radiation and *PAR* during the haze drought further decreased *ET*.

3.3 Drivers of net ecosystem CO_2-exchange

Modelled *NEE* from our *MLRM* simulated a small positive effect on *NEE* during the non-haze drought, with an increase in CO_2 uptake by 0.32 µmol m^{-2} s^{-1}, and a negative effect on *NEE* during the haze drought, with a decrease in CO_2 uptake by 0.99 µmol m^{-2} s^{-1} (Figure 6, Supplement Table S4). Modelled *NEE* is in good agreement with the measured *NEE*, i.e. for midday (10-14 h local time), nighttime (19-5:30 h) and average *NEE* (0-24 h) the model explains 98%, 94% and 83%, respectively, of the temporal variability in the measured *NEE*. Overall, the relative change of meteorological and environmental parameters during the non-haze drought and haze drought caused a more pronounced response of *NEE* in the latter period compared to non-drought and non-haze conditions, especially during midday (Figure 6).

During the non-haze drought, changes in radiation components were the main predictors of changes in midday *NEE*. Higher incoming *PAR* increased CO_2 uptake while at the same time, this gain in CO_2 uptake was compensated by the negative impact of decreasing fraction of diffuse radiation (Figure 6, Supplement Table S4). However, this estimated effect of the changes in irradiance on *NEE* was clearly small compared to the negative effects of dim light conditions during the haze drought where a reduction in incoming *PAR* resulted in strong decrease in CO_2 uptake (Figure 6). Further, the effect of incoming *PAR* and fraction of diffuse radiation on midday *NEE* was reversed during the haze drought compared to the non-haze drought and the decrease in fraction of diffuse radiation contributed to higher midday CO_2 uptake but these positive effects were almost offset completely by the decrease in incoming *PAR*.

Increasing *VPD* had a negative impact on midday *NEE* (decrease in CO_2 uptake), while the increase in air temperature had a positive impact on midday *NEE* (increase in CO_2 uptake). Oil palm drought stress, manifested in a general decrease in ET/ET_{pot}

(Table 2), was less severe during the non-haze drought compared to the haze drought period, resulting in a slightly more pronounced decrease in CO_2 uptake during the latter period (Figure 6). The observed changes in atmospheric CO_2 concentrations during the non-haze drought and haze drought suggest that the oil palm might respond via photosynthesis and stomata behaviour to the elevated atmospheric CO_2 levels. However, rising atmospheric CO_2 concentration had no fertilization effect for the oil palm plantation, in contrary, the increase in CO_2 concentration contributed to a decrease in CO_2 uptake (Figure 6).

During both non-haze drought and haze drought, the change in nighttime (19-5:30 h) air temperature above the canopy was the main predictor of changes in nighttime *NEE* (respiration). The increase in air temperature tended to increase respiration. This was more pronounced during the haze drought compared to the non-haze drought (Figure 6, Supplement Table S4 & S5).

3.4 *NEE* under intensified drought and haze conditions

Our two model projections, where we increased the effects of non-haze drought and haze drought conditions based on the 2015-drought and haze conditions, showed that increased non-haze drought conditions (*NHD+*) enhanced CO_2 uptake while increased haze drought (*HD+*) weakened CO_2 uptake and might even promote CO_2 release (Figure 7, Supplement Table S6). Daily average (24-hour) CO_2 uptake in *NHD+* was increased by 2.25 µmol m^{-2} s^{-1} compared to the 2015-non-haze drought conditions. *NHD+* might enhance midday CO_2 uptake and nighttime respiration, which increased by 6.52 µmol m^{-2} s^{-1}, 1.59 µmol m^{-2} s^{-1}, respectively, mainly due to the effect of a high air temperature in *NDH+* which is also the main predictor of daily average, midday and nighttime *NEE* (Supplement Table S6). Incoming *PAR* is the dominant light parameter for *NEE* and increases in incoming *PAR* in *NHD+* are able to offset the modelled negative impact of decreased fraction of diffuse radiation on *NEE*. This is contrary to what the model suggested for the 2015-non-haze drought reference conditions where we observe that the increase in incoming *PAR* was not able to offset the negative impacts on *NEE* due to decreased fraction of diffuse radiation. Similar to *NHD+*, air temperature in the increased haze drought scenario (*HD+*) was the main predictor of *NEE* and contributed to a high midday and daily average (24-hour) CO_2 uptake and also to a high nighttime respiration (Figure 7, Supplement, Table S7). However, the negative effects of *HD+* offset the positive effects of increased air temperature. Daily average (24-hour) CO_2 uptake and midday CO_2 uptake in *HD+* were decreased by 0.85 µmol m^{-2} s^{-1}, 4.51 µmol m^{-2} s^{-1}, respectively, while nighttime ecosystem respiration was increased by 2.53 µmol m^{-2} s^{-1}. Incoming *PAR* in *HD+* remains the dominant light parameter on midday *NEE* and its decrease cannot be offset by the positive effects of increased fraction of diffuse radiation. In *HD+*, midday *VPD* is of less relative importance on *NEE* as compared to the reference haze drought conditions. As already observed in the 2015-haze drought model output, increased CO_2 concentration in *HD+* does not act as an additional fertilization for the oil palm plantation. In contrast, the negative impact of increased CO_2 concentration on *NEE* becomes the dominant predictor of *NEE* in *HD+*. Our two scenarios indicate that increased drought stress, reflected by decreasing ET/ET_{pot}, has more pronounced negative impact on *NEE* in *HD+* compared to *NHD+*. However, oil palm seems to be relatively resistant against drought since the overall impact of changes in ET/ET_{pot} on *NEE* was relatively small in both scenarios.

Biogeosciences Discuss., https://doi.org/10.5194/bg-2019-49
Manuscript under review for journal Biogeosciences
Discussion started: 12 February 2019

4 Discussion

4.1 Oil palm response to drought and haze conditions

Oil palm has exceptionally high photosynthetic efficiency compared to most of the vascular plants (Apichatmeta et al., 2017) but this efficiency comes with a downside: Oil palm, like many other tropical plants, shows a distinct reaction to changes in atmospheric and soil parameters, with gradual symptoms of water and heat stress which directly affect photosynthesis and evapotranspiration as well as fruit bunch development and yield (Bakoumé et al., 2013; Paterson et al., 2013). During our study period, we observed that accumulated annual precipitation 2015 and during the reference period was on the lower limit of reported optimum precipitation range for oil palm (Pirker et al., 2016). However, oil palm requires minimum precipitation of 100 mm per month to avoid drought stress (Corley & Tinker, 2016). This was not fulfilled in September 2014, from June to October 2015, and in January 2016. In our study, however, we found no strong correlation between *NEE* and soil moisture conditions, and between *NEE* and ET/ET_{pot} during the non-haze drought and haze drought period which suggests that oil palm was relatively resistant against drying soil.

Temperature increase and related heat stress is another factor which might negatively affect the growth of oil palm (Oettli et al., 2018). Our analysis did not support this finding because during the non-haze drought the effect of increasing temperature on *NEE* was almost negligible. During the haze drought, higher air temperature had a positive impact on CO_2 uptake although the haze period experienced the highest air temperature during the entire study period.

Oil palm seems particularly susceptible to changes in atmospheric *VPD* (Lamade & Bouillet, 2005; Wahid et al., 2005; Bayona-Rodríguez & Romero, 2016; Mathews & Ardiyanto, 2016) with high levels of *VPD* causing partial closure of stomata and limiting photosynthesis and transpiration. Dufrene & Saugier (1993) found that *VPD* >17 hPa had a strong negative impact on CO_2 fluxes of oil palm. On a daily basis, this threshold was not reached during the non-haze drought which is likely to explain why *NEE* during that period seemed to be rather unperturbed by the steady increase in *VPD*. The haze drought, however, showed a different picture and *VPD* close to this reported threshold exerted a strong impact on *NEE*, with overall decrease in CO_2 uptake. To a certain extent, oil palm is capable to adjust its stomatal regulation to short-term periods of relatively low *VPD* and low soil water deficit by increasing its maximum rate of photosynthesis (A_{max}) (Dufrene & Saugier, 1993; Apichatmeta et al., 2017). However, during the non-haze drought and haze drought those two environmental parameters exerted only little impact on A_{max} and changes in irradiance seemed to be the dominant driver of A_{max}.

Oil palm grows in regions with high solar flux densities (Barcelos et al., 2015) and it is able to strategically optimize its photosynthesis to light conditions, with pronounced diurnal effects and maximum efficiency before or at about midday (Apichatmeta et al., 2017). In our study, measurements and *MLRM*-results showed strongest response of oil palm *NEE* to drought, haze and changes in irradiance during midday. Due to the reduction of incoming PAR for almost two months, the haze was a major and persistent disturbing factor for oil palm *NEE* and A_{max}. The initial increase in diffuse light conditions and its positive impact on Amax and *NEE* cannot compensate for the reduction in incoming *PAR*. Therefore, the observed pause

in carbon accumulation and even small carbon release during the haze drought could have been prevented since without the haze, the oil palm plantation would have remained a sink of CO_2 during that period.

Changes in oil palm yield are one direct consequence of varying meteorological and climatic conditions (Mathews & Ardiyanto, 2016; Oettli et al., 2018). Prolonged drought does not only affect carbon accumulation via photosynthesis but leads to abortion of female inflorescences and failing bunch yield (Bakoumé et al., 2013). Oil palm yield in 2016, and its initial sharp drop by the end of 2015 can therefore be related to the drought and haze conditions. Here, the haze was the driving stressor and similar to the effects of haze on *NEE*, without the haze oil palm yield might not have experienced such a sharp decline.

Short-term elevated CO_2 exposure on oil palm seedlings (Ibrahim et al., 2010; Jaafar & Ibrahim, 2012) and on mature oil palm (Henson & Harun, 2005) have shown that elevated CO_2 concentration promote plant growth due to elevated rates of photosynthesis and reduced water loss by transpiration. To our knowledge, no comprehensive study has investigated the complex interplay of elevated CO_2 concentrations, increased temperature and decrease in radiation in oil palm. Mathews & Ardiyanto (2016) speculate that short-term elevated levels of CO_2 under haze conditions and related potentially strong stomatal opening may offset for the lack of irradiance and related shorter timing of stomatal opening. Based on leaf gas exchange measurements in trees, Urban et al., (2014) come to a contradiction that low irradiance is incapable to activate stomatal opening since plants exposed to elevated CO_2 levels require higher stomatal activation energy. From our results, it is highly doubtable that elevated CO_2 exposure during the haze had any fertilization effect. On the contrary, increasing atmospheric CO_2 concentration acted as an additional stress factor for oil palm and decreased CO_2 uptake.

4.2 Future *ENSO* projections, oil palm response and adaptation strategies

Paterson et al., (2015) report that increasing frequency of drought in Southeast Asia has already caused a decline of 10-30% in palm oil production. Our study supports the findings of Dufrene & Saugier (1993) and Apichatmeta et al. (2017) that short-term drought conditions and elevated irradiance may be beneficial for oil palm growth since we observe an increase in CO_2 uptake during the non-haze drought despite relatively high *VPD* and low soil moisture content. Our scenario of increased non-haze drought (*NHD+*) suggests that drought conditions may enhance CO_2 uptake to a certain extent, mainly due to increased incoming *PAR* and increased air temperature. However, our scenario does not consider a temporal prolongation of the drought, only changes in magnitude of the atmospheric and environmental parameters. Therefore, we cannot rule out that this modelled positive effect of *NHD+* on CO_2 uptake can be maintained if drought conditions remain over a longer period but the relatively weak impact of ET/ET_{pot} on *NEE* suggests that oil palm is relatively resistant to drought.

The reduced irradiance due to fire-induced haze is another stressor for oil palm since it occurs during those periods when the oil palm plantation is already negatively affected by drought and heat. Similar to *NHD+*, we did not include temporal changes in the length of the increased haze drought scenario (*HD+*) but we see that *HD+* may amplify the negative impacts on oil palm *NEE*. Future negative impacts of *ENSO*-related droughts on oil palm productivity, carbon sequestration, growth and yield might therefore be strongly coupled with the temporal and spatial occurrence of fire-induced haze.

It has been shown that fertilized mature commercial oil palm plantations transpire more water than tropical rainforests due to high productivity (Manoli et al., 2018), thus making them more prone to the effects of droughts (Bakoumé et al., 2013). Adaptation strategies, such as short-term irrigation or the establishment of irrigation ditches may dampen the drought-related impacts in oil palm plantations but aggravate the depletion of natural water reservoirs (Manoli et al., 2018). Elongated periods of drought, as shown in this study, increase sensible heating at the cost of evapotranspiration, resulting in surface warming. Oil palm plantations have a strong potential to further amplify air heating during droughts since they are hotter and dryer as compared to tropical rainforest and rubber monocultures even during non-El Niño years (Hardwick et al., 2015; Meijide et al., 2018). Covering vast areas of tropical lowlands of Sumatra and Borneo, oil palm plantations have already caused an increase in land surface temperature (Sabajo et al., 2017).

State-of-the-art process-based land surface schemes, such as the Community Land Model (*CLM4*.5) (Oleson et al., 2013; Fan et al., 2015), are powerful tools to address ecosystem surface energy balance, hydrological processes and carbon-nitrogen biogeochemistry (Oleson et al., 2013; Fan et al., 2015). Although these models are well-developed and widely-used, they fail to include smoke haze as an environmental parameter affecting ecosystem behaviour. In this study, we used a simple multi linear regression model (*MLRM*) to assess the impact of haze drought on oil palm productivity and developed an increased haze scenario (*HD+*). With this simple model we were able to show strong site-specific negative response of oil palm to haze drought. These specific results of oil palm behaviour during drought and haze conditions might be useful to parameterize models, such as *CLM* and even applicable to other ecosystem and land-use types.

5 Conclusions

In this study, we investigate the impact of drought and smoke haze on the CO_2 exchange, evapotranspiration and surface energy budget in a commercial oil palm plantation. We found that drought and smoke haze conditions, with related increase in atmospheric *VPD* and air temperature, and changes in light conditions are major disturbing factors for the oil palm plantation. Drought conditions increased sensible heating at the cost of evapotranspiration while strong smoke haze resulted in a complete pause of carbon accumulation for 1.5 months with subsequent decline in oil palm yield. In general, our measurements and *MLRM* showed that the strong haze amplified the negative effects of the drought. It is very likely that without the haze, the negative impact on CO_2 fluxes, carbon accumulation and yield would have been less pronounced. Fire-preventing measures such as sustainable land management, stricter law enforcement and sanctioning, strategic hazard planning and awareness-raising on the effects of fires on oil palm yield but also on air quality and health may help to mitigate the negative effects of drought. Further, incorporating smoke haze as an environmental stress factor into regional or global model approaches may foster more accurate estimations of ecosystem CO_2, energy and water vapour flux behaviour during such extreme meteorological events and may allow a more holistic viewpoint of possible adaptation strategies and hazard-prevention caused by *ENSO*.

Code and data availability

The code and data used in this study are available on GitHub (https://github.com/CbioST/ENSO_OilPalm).

Author contribution

The original idea of the paper was suggested by Alexander Knohl (AK), Ana Meijide (AM) and Christian Stiegler (CS) and discussed and developed by all authors. AM performed the field work and CS performed the data analysis. Ashehad Ashween Ali (AA) and CS developed the model code, run the simulations and performed the model analysis. CS prepared the manuscript with contributions from all co-authors.

Acknowledgements

This study was funded by the Deutsche Forschungsgemeinschaft (DFG, German Research Foundation) – project number 192626868 – SFB 990 and the Ministry of Research, Technology and Higher Education (Ristekdikti) in the framework of the collaborative German - Indonesian research project CRC990, subproject A03 and A07. The authors wish to thank our local field assistants in Indonesia, i.e. Basri, Bayu and Darwis as well as Edgar Tunsch, Malte Puhan, Frank Tiedemann and Dietmar Fellert for technical support. We also thank PTPN6 for permission to conduct our research at the oil palm plantation.

References

Agus, F., Henson, I. E., Sahardjo, B. H., Harris, N., van Noordwijk, M., and Killeen, T.: Review of emission factors for assessment of CO2 emission from land use change to oil palm in Southeast Asia. Singapore: Roundtable on Sustainable Palm Oil, 2013.

Allen, K., Corre, M. D., Tjoa, A., and Veldkamp, E.: Soil Nitrogen-cycling responses to conversion of lowland forests to oil palm and rubber plantations in Sumatra, Indonesia. PLoS ONE, 10(7), e0133325. doi:10.1371/journal.pone.0133325, 215.

Apichatmeta, K., Sudsiri, C. J., and Ritchie, R. J.: Photosynthesis of oil palm (Elaeis guineensis). Scientia Horticulturae, 34-40. doi:10.1016/j.scienta.2016.11.013, 2017.

Bakoumé, C., Shahbudin, N., Yacob, S., Siang, C. S., and Thambi, M. N.: Improved method for estimating soil moisture deficit in oil palm (*Elaeis guineensis* Jacq.) areas with limited climatic data. Journal of Agricultural Science, 5(8), 57-65. doi:10.5539/jas.v5n8p57, 2013.

Barcelos, E., de Almeida Rios, S., Cunha, R. N., Lopes, R., Motoike, S. Y., Babiychuk, E., and Kushnir, S.: Oil palm natural diversity and the potential for yield improvement. Frontiers in Plant Science, 6(190). doi:10.3389/fpls.2015.00190, 2015.

Bayona-Rodríguez, C., and Romero, H. M.: Estimation of transpiration in oil palm (Elaeis guineensis Jacq.) with the heat ratio method. Agronomía Colombiana, 34(2), 172-178. doi:10.15446/agron.colomb.v34n2.55649, 2016.

Betts, R. A., Jones, C. D., Knight, J. R., Keeling, R. F., and Kennedy, J. J.: El Niño and a record CO_2 rise. Nature Climate Change, 6, 806-810, 2016.

Cai, W., Borlace, S., Lengaigne, M., van Resch, P., Collins, M., Vecchi, G., and Jin, F.-F.: Increasing frequency of extreme El Niño eventsdue to greenhouse warming. Nature Climate Change, 111-116. doi: 10.1038/NCLIMATE2100, 2014.

Cai, W., Wang, G., Dewitte, B., Wu, L., Santoso, A., Takahashi, K., and McPhaden, M.: Increased variability of eastern Pacific El Niño under greenhouse warming. Nature, 564, 201-206. doi:10.1038/s41586-018-0776-9, 2018.

Caliman, J., and Southworth, A.: Effect of drought and haze on the performance of oil palm. 1998 International Oil Palm Conference. Commodity of the past, today, and the future, (pp. 1-40). Sheraton Nusa Indah Hotel, Bali, 1998.

Cao, H.-X., Sun, C.-X., Shao, H.-B., and Lei, X.-T.: Effects of low temperature and drought on the physiological and growth changes in oil palm seedlings. African Journal of Biotechnology, 10(14), 2630-2637. doi:10.5897/AJB10.1272, 2011.

Chatfield, C.: Problem Solving: a Statistician's Guide. London: Chapman and Hall, 1995.

Chen, G., Hobbie, S. E., Reich, P. B., Yang, Y., and Robinson, D.: Allometry of fine roots in forest ecosystems. Ecology Letters. doi:10.1111/ele.13193, 2018.

Chong, K. L., Kanniah, K. D., Pohl, C., and Tan, K. P.: A review of remote sensing applications for oil palm studies. Geo-spatial Information Science, 20, 184-200. doi:10.1080/10095020.2017.1337317, 2017.

Corley, R. H., and Tinker, P. B.: The Oil Palm. Chichester, West Sussex, UK: Wiley-Blackwell, 2016.

Drescher, J., Rembold, K., Allen, K., Beckschäfer, P., Buchori, D., Clough, Y., and Scheu, S.: Ecological and socio-economic functions across tropical land use systems after rainforest conversion. Philosophical Transactions B, 371, 20150275. doi:10.1098/rstb.2015.0275, 2016.

Dufrene, E., and Saugier, B.: Gas exchange of oil palm in relation to light, vapour pressure deficit, temperature and leaf age. Functional Ecology, 7, 97-104, 1993.

Falge, E., Baldocchi, D., Olson, R., Anthoni, P., Aubinet, M., Bernhofer, C., and Wofsy, S.: Gap filling strategies for defensible annual sums of net ecosystem exchange. Agricltural and Forest Meteorology, 107, 43-69, 2001.

Fan, Y., Roupsard, O., Bernoux, M., Le Maire, G., Panferov, O., Kotowska, M. M., and Knohl, A.: A sub-canopy structure for simulating oil palm in the Community Land Model (CLM-Palm): Phenology, allocation and yield. Geoscientific Model Development, 8, 3786-3800. doi:10.5194/gmd-8-3785-2015, 2015.

Hardwick, S. R., Toumi, R., Pfeifer, M., Turner, E. C., Nilus, R., and Ewers, R. M.: The relationship between leaf area index and microclimate in tropical forest and oil palm plantation: Forest disturbance drives changes in microclimate. Agricultural and Forest Meteorology, 201, 187-195. doi:10.1016/j.agrformet.2014.11.010, 2015.

Henson, I. E.: Modelling the effects of 'haze' on oil palm poductivity and yield. Journal of Oil Palm Research, 12(1), 123-134, 2000.

Henson, I. E., and Harun, M. H.: Carbon dioxide enrichment in oil palm canopies and its possible influence on photosynthesis. Oil Palm bulletin, 10-19, 2005.

Henson, I. E., and Harun, M. H.: The influence of climatic conditions on gas and energy exchanges above a yoooung oil palm stand in North Kendah, Malaysia. Journal of Oil Palm Research, 17, 73-91, 2005.

Heuvelink, T. L., Dueck, T. A., Janse, J., Gort, G., and Marcelis, L. F.: Enhancement of crop photosynthesis by diffuse light: quantifying the contributing factors. Annals of Botany, 114, 145-156. doi:10.1093/aob7mcu071, 2014.

Huijnen, V., Wooster, M. J., Kaier, J. W., Gaveau, D. L., Flemming, J., Parrington, M., and van Weele, M.: Fire carbon emissions over maritime southeast Asia in 2015 largest since 1997. Scientific Reports, 26886. doi:10.1038/srep26886, 2016.

Ibrahim, M. H., Jaafar, H. Z., Harun, M. H., and Yusop, M. R.: Changes in growth and photosynthetic patterns of oil palm (Elaeis guineensis Jacq.) seedlings exposed to short-term CO2 enrichment in a closed top chamber. Acta Physiol Plant, 32, 305-313, 2010.

IPCC: Climate Change 2013: The physical science basis. Contribution of working group I to the fifth assessment report of the intergovernmental panel on cliamate change. (T. F. Stocker, D. Qin, G.-K. Plattner, and P. M. Midgley, Eds.) Cambridge: Cambridge University Press. doi:10.1017/CBO9781107415324, 2013.

Jaafar, H. Z., and Ibrahim, M. H.: Photosynthesis and quantum yield of oil palm juveniles to elevated carbon dioxide. In M. M. Najafpour (Ed.), Advances Photosynthesis Fundamental Aspects (pp. 321-340). Rijeka: InTechPubl. doi:10.5772/26167, 2012.

Jazayeri, S. M., Rivera, Y. D., Camperos-Reyes, J. E., and Romero, H. M.: Physiological effects of water deficit on two oil palm (Elaeis guineensis Jacq.) genotypes. Agronomia Colombiana, 33(2), 164-173. doi:10.15446/agron.colomb.v33n2.49846, 2015.

Jiménez-Muñoz, J. C., Mattar, C., Barichivich, J., Santamaria-Artigas, A., Takahashi, K., Malhi, Y., and Schrier, G.: Record-breaking warming and extreme drought in the Amazon rainforest during the course of El Niño 2015-2016. Scientific Reports, 6, 33130, 2016.

Kanniah, K. D., Beringer, J., North, P., and Hutley, L.: Control of atmospheric particles on diffuse radiation and terrestrial plant productivity: A review. Progress in Physical Geography, 36(2), 209-237. doi:10.1177/0309133311434244, 2012.

Keupp, L., Pollinger, F., and Paeth, H.: Assessment of future ENSO changes in a CMIP3/CMIP5 multi-model and multi-index framework. International Journal of Climatology, 3439-3451. doi:10.1002/joc.4928, 2017.

Kim, S. T., Cai, W., Jin, F.-F., Santoso, A., Wu, L., and Guilyardi, E.: Response of El Niño sea surface temperature variability to greenhouse warming. Nature Climate Change, 786-790. doi:10.1038/NCLIMATE2326, 2014.

Knohl, A., and Baldocchi, D. D.: Effects of diffuse radiation on canopy gas exchange processes in a forest ecosystem. Journal of Geophysical Research, 113, G02023. doi:10.1029/2007JG000663, 2008.

Koh, L. P., and Ghazoul, J.: Biofuels, bodiversity, and people: Understanding the conflicts and finding opportunities. Biological Conservation, 141, 2450-2460. doi:10.1016/j.biocon.2008.08.005, 2008.

Koh, L. P., Miettinen, J., Liew, S. C., and Ghazoul, J.: Remotely sensed evidence of tropical peatland conversion to oil palm. Proceedings of the National Academy of Sciences, 108(12), 5127-5132. doi:10.1073/pnas.1018776108, 2011.

Kotowska, M. M., Leuschner, C., Triadiati, T., Meriem, S., and Hertel, D.: Quantifying above- and belowground biomass carbon loss with forest conversion in tropical lowlands of Sumatra (Indonesia). Global Change Biology, 21, 3620-3634. doi:10.1111/gcb.12979, 2015.

Kozlov, V. S., Yausheva, E. P., Terpugova, S. A., Panchenko, M. V., Chernov, D. G., and Shmargunov, V. P.: Optical-microphysical properties of smoke haze from Siberian forest fires in summer 2012. International Journal of Remote Sensing, 35(15), 5722-5741. doi:10.1080/01431161.2014.945010, 2014.

Kozlowski, T., and Pallardy, S.: Photosynthesis. In T. Kozlowski, and S. Pallardy, Physiology of woody plants (2 ed., pp. 87-132). San Diego: Academic Press., 1997.

Lamade, E., and Bouillet, J.-P.: Carbon storage and global change: the role of oil palm. Oilseeds and fats, Crops and Lipids, 12(2), 154-160, 2005.

Legros, S., Mialet-Serra, I., Caliman, J.-P., Siregar, F. A., Clément-Vidal, A., and Dingkuhn, M.: Phenology and growth adjustments of oil palm (Elaeis guineensis) to photoperiod and climate variability. Annals of Botany, 104, 1171-1182. doi:10.1093/aob/mcp214, 2009.

Lim, Y.-K., Kovach, R. M., Pawson, S., and Vernieres, G.: The 2015/16 El Niño event in context of the MERRA-2 reanalysis: a comparison of the tropical Pacific with 1982/83 and 1997/98. Journal of Climate, 30, 4819-4842. doi:10.1175/JCLI-D-16-0800.1, 2017.

Maillard, G., Ochs, R., and Daniel, C.: Analysis of the effects of drought on the oil palm. Oleagineux, 29(8-9), 397-404, 1974.

Manoli, G., Meijide, A., Huth, N., Knohl, A., Kosugi, Y., Burlando, P., and Fatichi, S.: Ecohydrological changes after tropical forest conversion to oil palm. Environmental Research Letters, 13, 064035. doi:10.1088/1748-9326/aac54e, 2018.

Mathews, J., and Ardiyanto, A.: Impact of forest fire induces haze on oil extraction rate (OER) in Central Kalimantan province. Journal of Oil Palm, Environment and Health, 7, 28-33. doi:10.5366/jope.2016.03, 2016.

Meijide, A., Badu, C. S., Moyano, F., Tiralla, N., Gunawan, D., and Knohl, A.: Impact of forest conversion to oil palm and rubber plantations on microclimate and the role of the 2015 ENSO event. Agricultural and Forest Meteorology, 252, 208-219. doi:10.1016/j.agrformet.2018.01.013, 2018.

Meijide, A., Röll, A., Fan, Y., Herbst, M., Niu, F., Tiedemann, F., and Knohl, A.: Controls of water and energy fluxes in oil palm plantations: Environmental variables and oil palm age. Agricultural and Forest Meteorology, 239, 71-85. doi:10.1016/j.agrformet.2017.02.034, 2017.

Moreira, D. S., Longo, K. M., Freitas, S. R., Yamasoe, M. A., Mercado, L. M., Rosário, N. E., and Correia, C. C.: Modeling the radiative effects of biomass burning aerosols on carbon fluxes in the Amazon region. Atmospheric Chemistry and Physics, 14785-14810. doi:10.5194/acp-17-14785-2017, 2017.

Neelin, J. D., Münnich, M., Su, H., Meyerson, J. E., and Holloway, C. E.: Tropical drying trends in global warming models and observations. Proceedings of the National Academy of Sciences, 103, 6110-6115, 2006.

Noor, M. R., Harun, M. H., and Jantan, N. M.: Physiological plant stress and responses in oil palm. Oil Palm Bulletin, 62, 25-32, 2011.

Oettli, P., Behera, S. K., and Yamagata, T.: Climate based predictability of oil palm tree yield in Malaysia. Scientific Reports, 8, 2271. doi:10.1038/s41598-018-20298-0, 2018.

Olchev, A., Ibrom, A., Panferov, O., Gushchina, D., Kreilein, H., Popov, V., Knohl, A.: Response of CO_2 and H_2O fluxes in a mountainous tropical rainforest in equatorial Indonesia to El Niño events. Biogeosciences, 12, 6655-6667. doi:10.5194/bg-12-6655-2015, 2015.

Oleson, K. W., Lawrence, D. M., Bonan, G. B., Drewniak, B., Huang, M., Koven, C. D., and Yang, Z.-L.: Technical description of version 4.5 of the Community Land Model (CLM). Boulder: National Center for Atmospheric Research. doi:10.5065/D6RR1W7M, 2013.

Paterson, R., Kumar, L., Shabani, F., and Lima, N.: World climate suitability projections to 2050 and 2100 for growing oil palm. Journal of Agricultural Science, 155, 689-702. doi:10.1017/S0021859616000605, 2017.

Paterson, R., Kumar, L., Taylor, S., and Lima, N.: Future climate effects on suitability for growth of oil palms in Malaysia and Indonesia. Scientific Reports, 5(14457). doi:10.1038/srep14457, 2015.

Paterson, R., Sariah, M., and Lima, N.: How will climate change affect oil palm fungal diseases? Crop Protection, 46, 113-120. doi:10.1016/j.cropro.2012.12.023, 2013.

Pirker, J., Mosnier, A., Kraxner, F., Havlík, P., and Obersteiner, M.: What are the limits to oil palm expansion? Global Environmental Change, 40, 73-81. doi:10.1016/j.gloenvcha.2016.06.007, 2016.

Power, S., Delage, F., Chung, C., Kociuba, G., and Keay, K.: Robust twenty-first-century projections of El Niño and related precipitation variability. Nature, 502, 541-547. doi:10.1038/nature12580, 2013.

Rasmusson, E. M., and Carpenter, T. H.: Variations in tropical sea surface temperature and surface wind fields associated with the Southern Oscillation/El Nino. Monthly Weather Review, 110, 354-384, 1981.

Ray-Mukherjee, J., Nimon, K., Mukherjee, S., Morris, D. W., Slotow, R., and Hamer, M.: Using commonality analysis in multiple regressions: a tool to decompose regression effects in the face of multicollinearity. Methods in Ecology and Evolution, 5, 320-328. doi:10.1111/2041-210x.12166, 2014.

Rivera Méndez, Y. D., Chacón, L. M., Bayona, C. J., and Romero, H. M.: Physiological response of oil palm interspecific hybrids (Elaeis oleifera H.B.K. Cortes versus Elaeis guineensis Jacq.) to water deficit. Brazilian Society of Plant Physiology, 24(4), 273-280, 2012.

Rowland, L., da Costa, A. C., Galraith, D. R., Oliveira, R. S., Binks, O. J., Oliveira, A. A., Meir, P.: Death from drought in tropical forests is triggere by hydraulics not carbon starvation. Nature, 528(119), 2015.

Sabajo, C. R., le Maire, G., June, T., Meijide, A., Roupsard, O., and Knohl, A.: Expansion of oil palm and other cash crops causes an increase of the land surface temperature in teh Jambi province in Indonesia. Biogeosciences, 14, 4619-4635. doi:10.5194/bg-14-4619-2017, 2017.

Santoso, A., Mcphaden, M. J., and Cai, W. (2017). The defining characteristics of ENSO extremes and the strong 215/2016 El Niño. Reviews of Geophysics, 55, 1079-1129. doi:10.1002/2017/RG000560, 2017.

Tangang, F. (2010). Climate change: is Southeast Asia up to the challenge?: the roles of climate variability and climate change on smoke haze occurrences in Southeast Asia region. (N. Kitchen, Ed.) London: London School of Economics and Political Science, 2010.

Turner, P. A., Field, C. B., Lobell, D. B., Sanchez, D. L., and Mach, K. J.: Unprecedented rates of land-use transformation in modelled climate cange mitigation pathways. Nature Sustainability, 1, 240-245. doi:10.1038/s41893-018-0063-7, 2018.

Urban, O., Klem, K., Holišová, P., Šigut, L., Šprtová, M., Teslová-Navrátilová, P., and Grace, J.: Impact of elevated CO2 concentration on dynamics of leaf photosynthesis in Fagus sylvatica is modulated by sky conditions. Environmental Pollution, 185, 271-280. doi:10.1016/j.envpol.2013.11.009, 2014.

USDA: Oilseeds: World markets and trade. Foreign Agricultural Service, United States Department of Agriculture. Washington: United States Department of Agriculture. Retrieved March 7, 2018, from https://apps.fas.usda.gov/psdonline/circulars/oilseeds.pdf, 2018.

Wahid, M. B., Abdullah, S. N., and Henson, I.: Oil palm- achievements and potential. Plant Production Science, 8(3), 288-297. doi:10.1626/pps.8.288, 2005.

Whittingham, M. J., Stephens, P. A., Bradbury, R. B., and Freckleton, R. P.: Why do we still use stepwise modelling in ecology and behaviour? Journal of Animal Ecology, 1182-1189. doi:10.1111/j.1365-2656.2006.01141.x, 2006.

Woittiez, L. S., van Wijk, M. T., Slingerland, M., van Noordwijk, M., and Giller, K. E.: Yields in oil palm: A quantitative review of contributing factors. European Journal of Agronomy, 83, 57-77. doi:10.1016/j.eja.2016.11.002, 2017.

Wolter, K.: The Southern Oscillation in surface circulation and climate over the tropical Atlantic, eastern Pacific, and Indian Oceans as captured by cluster analysis. Journal of Climate and Appled Meteorology, 26, 540-558, 1986.

Wolter, K., and Timlin, M. S.: El Niño/Southern Oscillation behaviour since 1871 as diagnosed in an extended multivariate ENSO index (MEI.ext). International Journal of Climatology, 31, 1074-1087. doi:10.1002/joc.2336, 2011.

Yamasoe, M. A., von Randow, C., Manzi, A. O., Schafer, J. S., Eck, T. F., and Holben, B. N.: Effect of smoke and clouds on the transmissivity of photosynthetically active radiation inside the canopy. Atmospheric chemistry and Physics, 6, 1645-1656, 2006.

Zhou, Z., Jiang, L., Du, E., Hu, H., Li, Y., Chen, D., and Fang, J.: Temperature and substrate availability regulate soil respiration in the tropical mountain rainforests, Hainan Island, China. Journal of Plant Ecology, 6(5), 325-334, doi:10.1093/jpe/rtt034, 2013.

Zuur, A. F., Ieno, E. N., and Elphick, C. S.: A protocol for data exploration to avoid common statistical problems. Methods in Ecology and Evolution, 3-14. doi:10.1111/j.2041-210X.2009.00001.x, 2010.

Biogeosciences Discuss., https://doi.org/10.5194/bg-2019-49
Manuscript under review for journal Biogeosciences
Discussion started: 12 February 2019

Figures

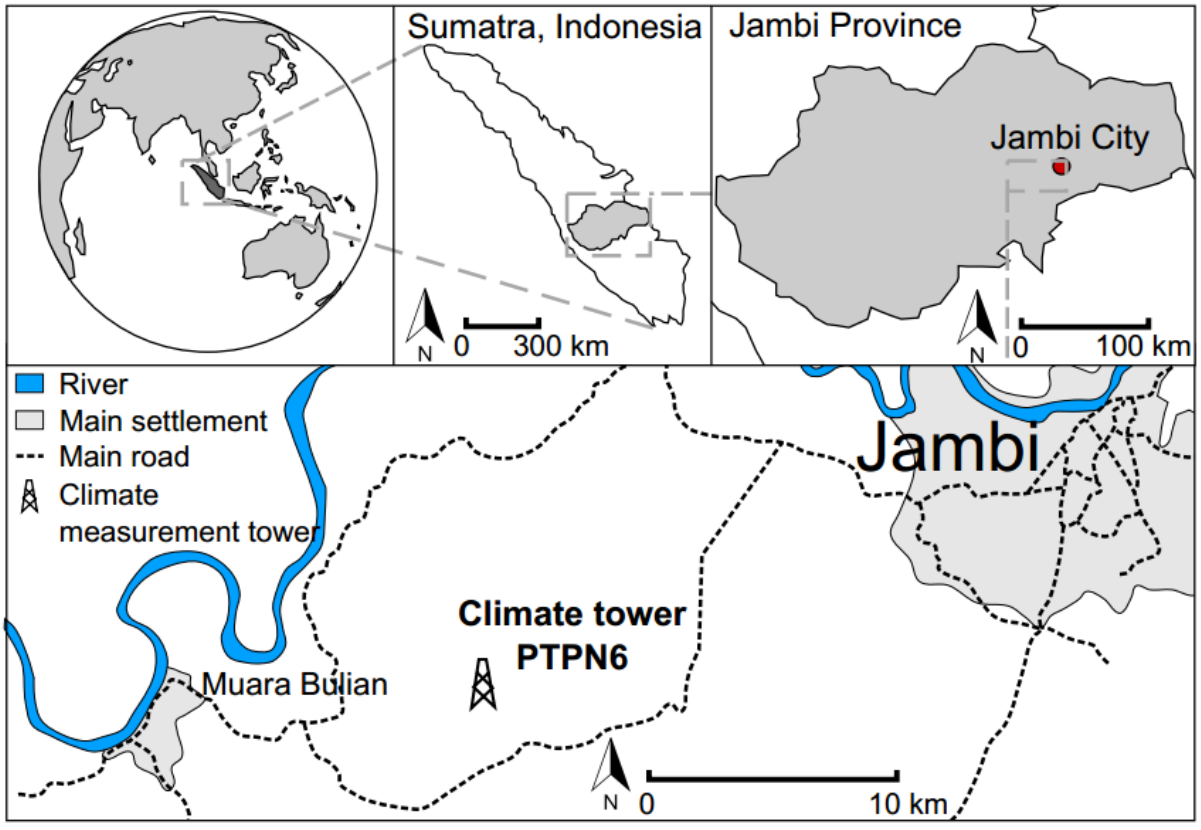

Figure 1: Map and location of the study site and climate measurement tower at PTPN6 oil palm plantation, approx. 15 km south-west of the city of Jambi (Sumatra, Indonesia)

Biogeosciences Discuss., https://doi.org/10.5194/bg-2019-49
Manuscript under review for journal Biogeosciences
Discussion started: 12 February 2019

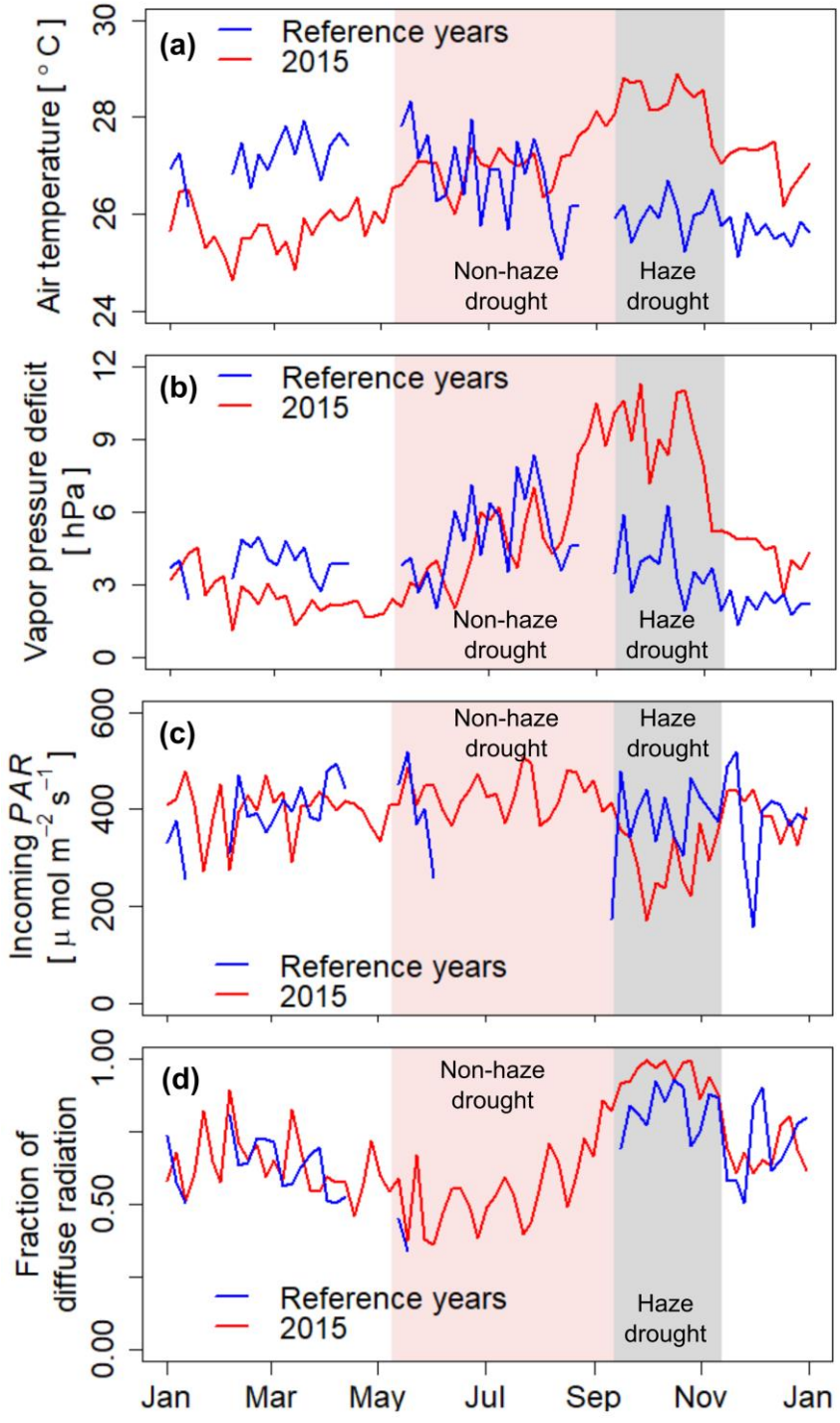

Figure 2: Five-day running mean of air temperature (a), atmospheric vapour pressure deficit (*VPD*) (b), incoming photosynthetically active radiation (*PAR*) (c), and fraction of diffuse radiation (d) during 2015 and the reference time period. Shaded areas in red and grey mark the non-haze drought and the haze drought period in 2015, respectively.

Biogeosciences Discuss., https://doi.org/10.5194/bg-2019-49
Manuscript under review for journal Biogeosciences
Discussion started: 12 February 2019

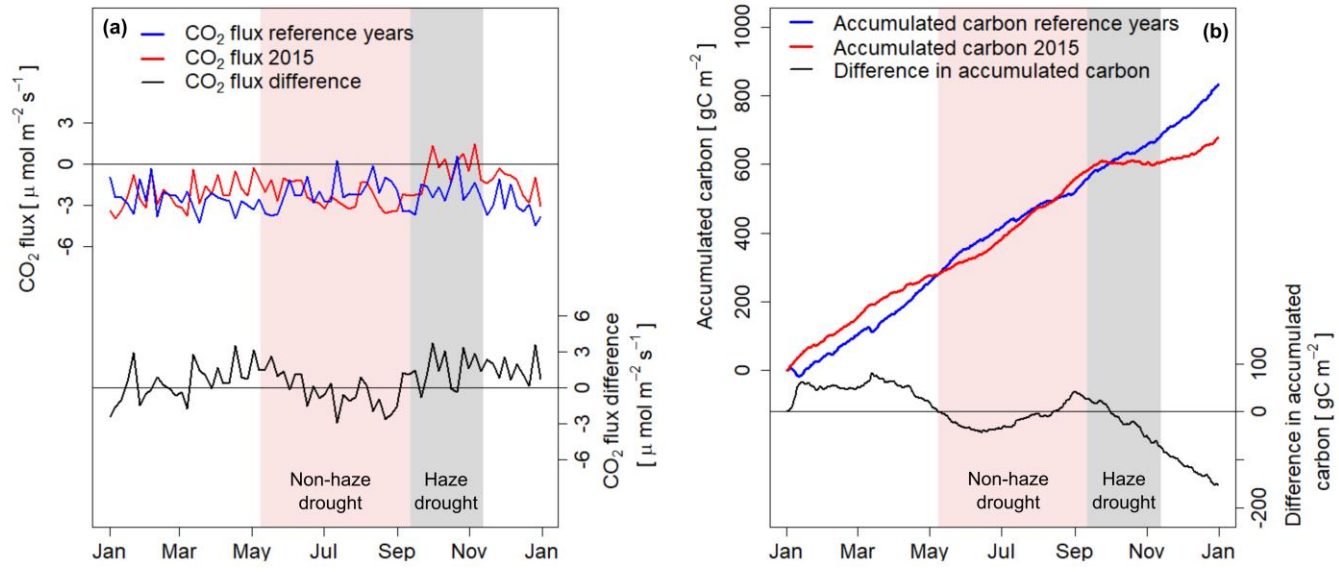

Figure 3: (a) Five-day running mean of net ecosystem CO_2-exchange (*NEE*) during 2015 and the reference time period and five-day running mean of CO_2 flux difference (2015 minus reference time period). (b) Accumulated carbon derived from CO_2 fluxes during the period 2015 and the reference time period, and differences in accumulated carbon between the two periods (2015 minus reference time period). Shaded areas in red and grey mark the non-haze drought and the haze drought period in 2015, respectively.

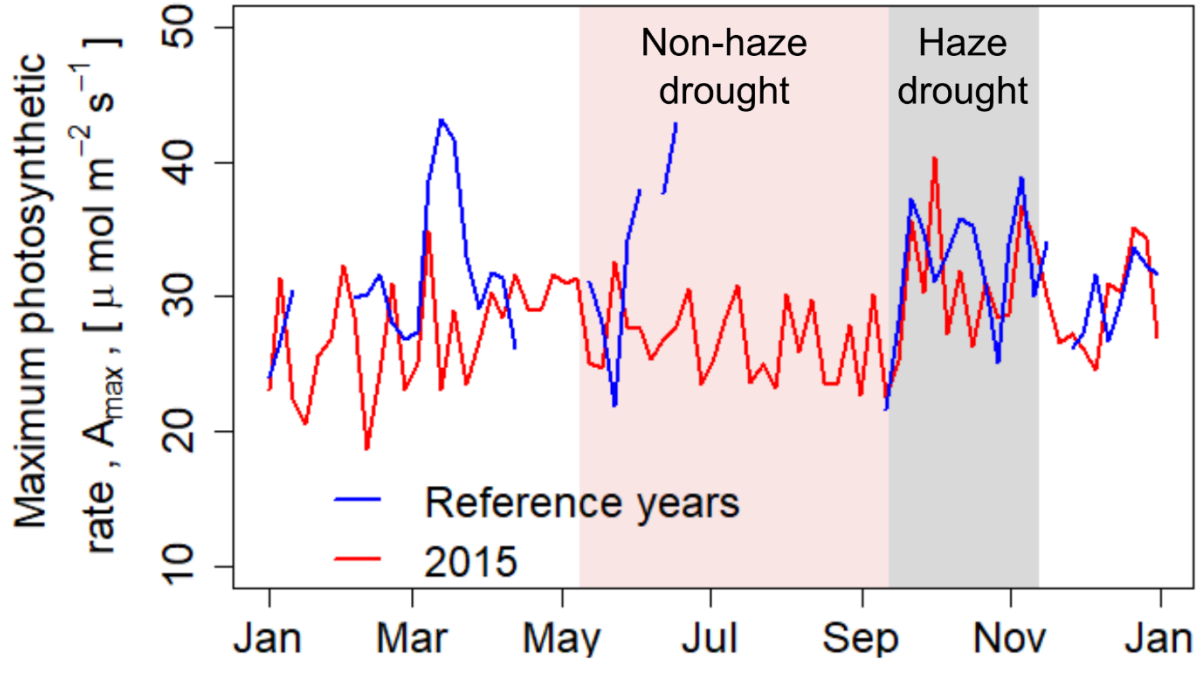

Figure 4: Five-day running mean of maximum rate of photosynthesis (A_{max}) during 2015 and during the reference time period. Sign convention has been performed to avoid negative values of A_{max}. Shaded areas in red and grey mark the non-haze drought and the haze drought period in 2015, respectively.

Biogeosciences Discuss., https://doi.org/10.5194/bg-2019-49
Manuscript under review for journal Biogeosciences
Discussion started: 12 February 2019

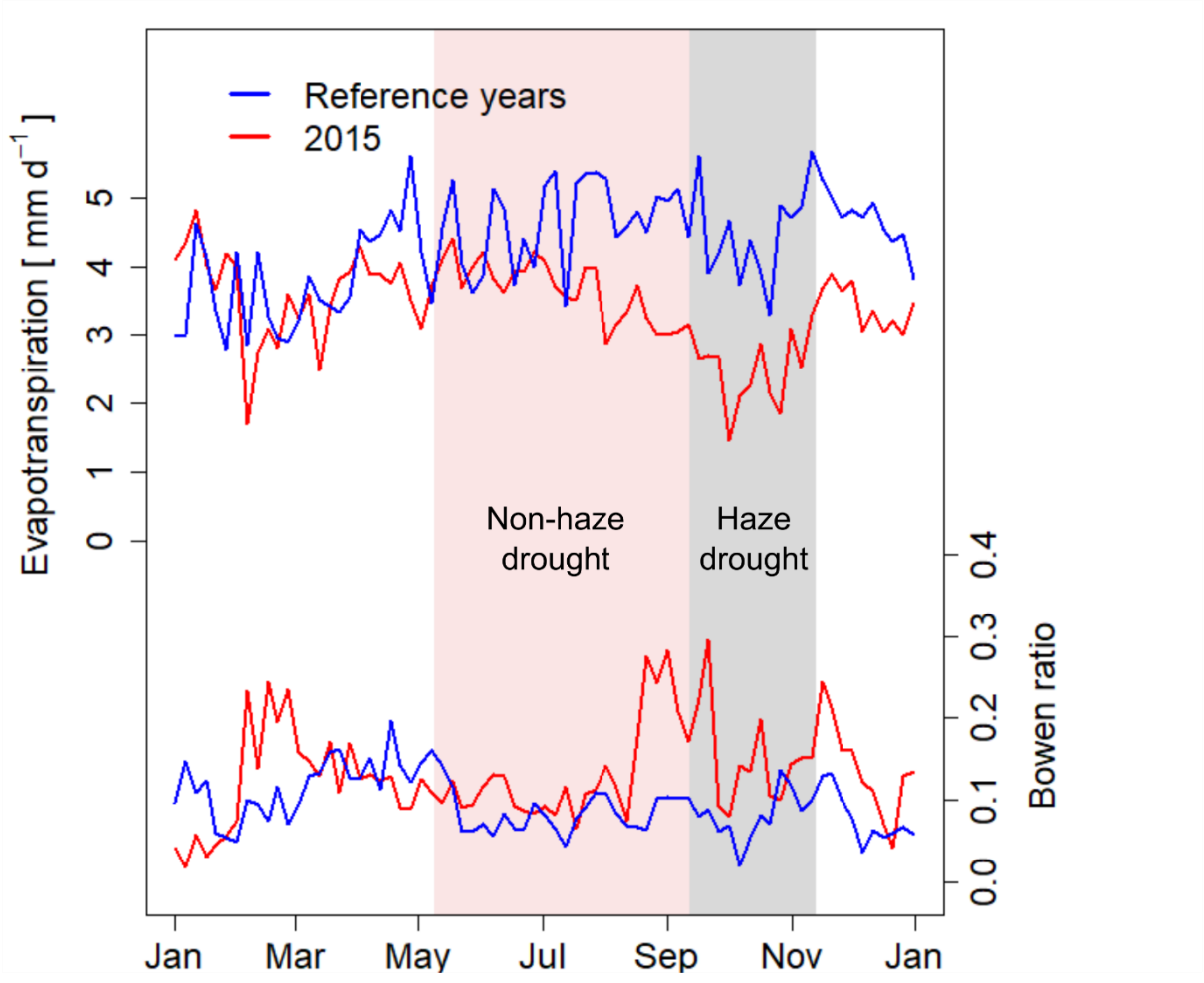

Figure 5: Five-day running mean of daily evapotranspiration and ratio of sensible to latent heat fluxes (Bowen ratio) during 2015. Shaded areas in red and grey mark the non-haze drought and the haze drought period in 2015, respectively.

Biogeosciences Discuss., https://doi.org/10.5194/bg-2019-49
Manuscript under review for journal Biogeosciences
Discussion started: 12 February 2019

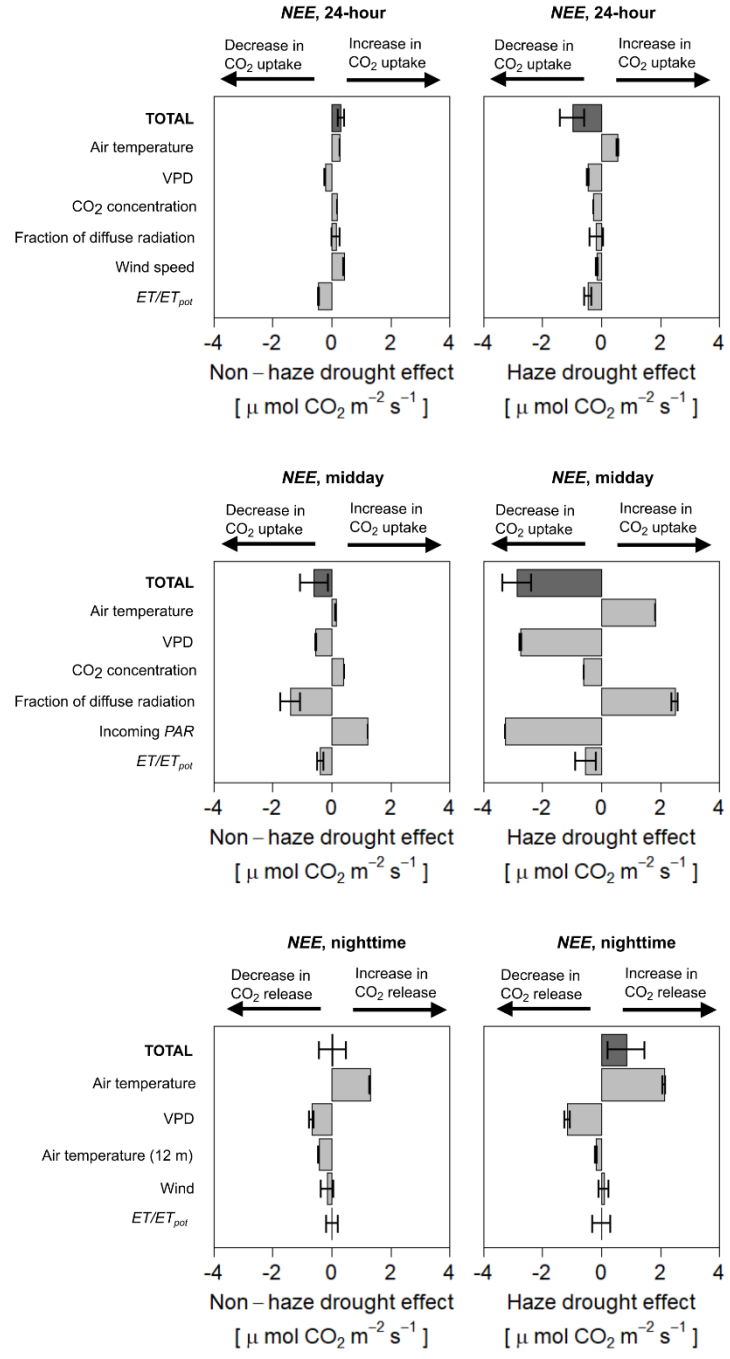

Figure 6: Contribution and effect of meteorological and environmental parameters during the non-haze drought and haze drought period on 24-hour (upper), midday (middle) and nighttime (lower) net ecosystem CO_2 exchange (*NEE*) compared to non-drought and non-haze conditions using Multiple Linear Regression Model (*MLRM*). Error bars show the standard error.

Biogeosciences Discuss., https://doi.org/10.5194/bg-2019-49
Manuscript under review for journal Biogeosciences
Discussion started: 12 February 2019

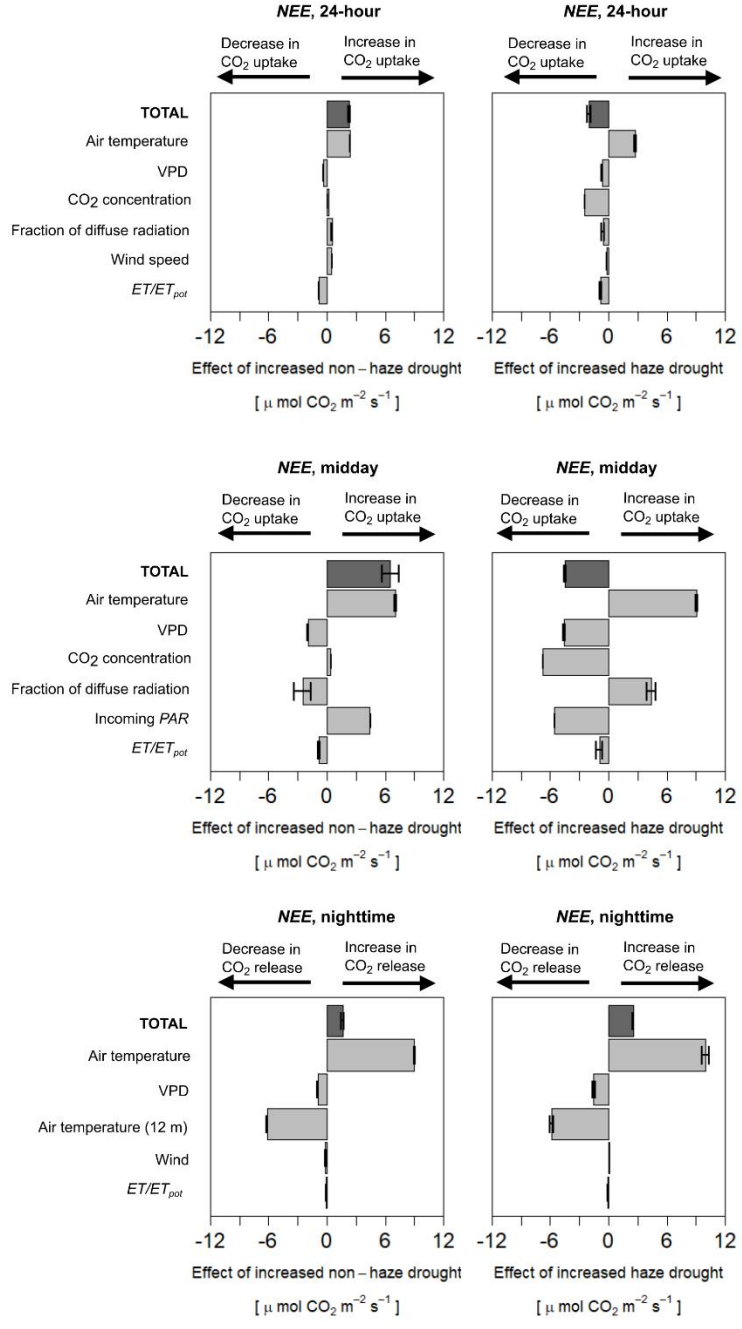

Figure 7: Contribution and effect of meteorological and environmental parameters considering increased non-haze drought (*NHD+*) and increased haze drought (*HD+*) scenario on 24-hour (upper), midday (middle) and nighttime (lower) net ecosystem CO_2 exchange (*NEE*) using Multiple Linear Regression Model (*MLRM*). Error bars show the standard error.

Biogeosciences Discuss., https://doi.org/10.5194/bg-2019-49
Manuscript under review for journal Biogeosciences
Discussion started: 12 February 2019

Tables

Table 1: Meteorological parameters (daily mean ± SD, or accumulated for precipitation and carbon) derived from 30-minute averages or sums during pre-drought, non-haze drought, haze drought and post-haze period in 2015, for the entire year 2015 and the reference period (May 2014-December 2014, January 2016-July 2016).

Period	Air temperature [°C]	Precipitation [mm]	Vapor pressure deficit (*VPD*) [hPa]	Soil moisture, 30 cm depth [vol%]	Soil moisture, 60 cm depth [vol%]	Soil moisture, 100 cm depth [vol%]	Incoming *PAR* [µmol m^2s^{-1}]	Fraction of diffuse radiation	Sunshine duration [hours d^{-1}]
Pre-drought (128 days)	25.7 ± 0.7	1003	2.53 ± 1.25	32.5 ± 1.8	31.9 ± 1.4	32.3 ±0.8	396.9 ± 105.0	0.67 ± 0.19	6.7 ± 6.9
Drought (127 days)	27.1 ± 0.7	192	5.30 ± 2.60	27.9 ± 4.3 [A)]	26.8 ±4.3 [B)]	27.1 ±2.9	432.0 ± 70.6	0.57 ± 0.18	10.0 ± 7.1

Haze (61 days)	28.3 ± 0.8	127	8.71 ± 2.57	18.1 ± 1.5	17.5 ± 0.2	24.4 ±0.1	293.2 ±97.3	0.95 ± 0.07	0.8 ± 3.2
Post-haze (49 days)	27.1 ± 0.9	608	4.30 ± 1.45	23.4 ± 1.3 C)	20.6 ±1.9 C)	26.8 ±2.1	393.8 ± 111.0	0.71 ± 0.17	6.0 ± 6.8
2015	26.8 ± 1.2	1930	4.76 ± 2.96	27.2 ±6.1	26.4 ±6.2	28.4 ±3.6	391.4 ± 104.7	0.69 ± 0.21	6.8 ± 7.2
Reference period	26.5 ± 1.1 D)	2030	4.0 ± 2.0 D)	28.3 ± 1.7 E)	29.9 ± 1.8 F)	25.5 ± 2.0 E)	397.6 ± 103.6 G)	-	-

A) no data 26.07.-06-09.2015, B) no data 05.08.-06.09.2015, C) no data 14.12.-31.12.2015, D) no data 30.08.-0.09.2014, 12.01.04.02.2016, 14.04.-11.05.2016, E) no data 31.05.-10.09.2014, 01.01.-04.02.2016, 14.04.11.05.2016, F) no data 31.05.-10.09.2014, 01.01.-11.02.2016, 14.04.-11.05.2016, G) no data 31.05.-08.09.2014, 12.01.-04.02.2016, 14.04.-11.05.2016

Biogeosciences Discuss., https://doi.org/10.5194/bg-2019-49
Manuscript under review for journal Biogeosciences
Discussion started: 12 February 2019

Table 2: Net CO_2 flux, maximum rate of photosynthesis (A_{max}), accumulated carbon, atmospheric CO_2-concentration, Bowen ratio, evapotranspiration (ET) and actual ET divided by potential ET (ET/ET_{pot}) (daily mean ± SD, or accumulated for precipitation and carbon) derived from 30-minute averages or daily average (A_{max}, Bowen ratio) during pre-drought, non-haze drought, haze drought and post-haze period in 2015, for the entire year 2015 and the reference period May 2014-December 2014, January 2016-July 2016.

Period	Net CO_2 flux (net ecosystem exchange) [µmol m^{-2} s^{-1}]	Maximum rate of photosynthesis (A_{max}) [µmol m^{-2} s^{-1}]	Accumulated carbon [g C m^{-2}]	CO_2 concentration [ppm]	Bowen ratio	Evapotranspiration (ET) (mm d^{-1})	ET/ET_{pot}
Pre-drought (128 days)	-2.10 ± 12.91	27.4 ± 8.1	278.6 ± 81.8	416 ± 29	0.12 ± 0.10	3.6 ± 4.9	0.55 ± 0.11
Drought (127 days)	-2.33 ± 14.07	26.6 ± 5.1	306.8 ± 91.1	412 ± 25	0.13 ± 0.13	3.7 ± 4.8	0.45 ± 0.09
Haze (61 days)	-0.33 ± 12.70	31.4 ± 8.3	23.0 ± 5.5	429 ± 26	0.16 ± 0.14	2.5 ± 3.5	0.45 ± 0.07
Post-haze (49 days)	-1.41 ± 14.50	29.1 ± 6.6	69.1 ± 20.0	429 ± 29	0.14 ± 0.14	3.4 ±4.6	0.48 ± 0.11
2015	-1.79 ± 13.53	28.0 ± 7.2	676.6± 199.2	418 ± 28	0.13 ± 0.12	3.4 ± 4.6	0.49 ± 0.11
Reference period	-2.20 ± 14.48	31.8 ± 8.4 G)	829.3 ± 242.3	407± 30	0.09 ± 0.05	4.3 ± 5.5	0.59 ± 0.15

G) no data 31.05.-08.09.2014, 12.01.-04.02.2016, 14.04.-11.05.2016